

Double shadow of a 4D Einstein-Gauss-Bonnet black hole and the connection between them with quasinormal modes

Tian-Tian Liu, He-Xu Zhang, Yu-Hang Feng, Jian-Bo Deng, and Xian-Ru Hu*

Institute of Theoretical Physics & Research Center of Gravitation,

Lanzhou University, Lanzhou 730000, China

Abstract

In this paper, we study the shadow of a 4D Einstein-Gauss-Bonnet black hole as photons couple to the Weyl tensor and find that the propagation of light depends on its polarization which leads to the existence of a double shadow. Then, we discuss the effect of the coupling parameter λ , the polarization of light and the Gauss-Bonnet coupling constant α on the shadow. Further we explore the influence of the Gauss-Bonnet coupling constant α on the quasinormal modes (QNMs) of massless scalar field and investigate the connection between the real part of QNMs in the eikonal limit and the shadow radius of black holes. We find that in the eikonal limit the real part of QNMs is inversely proportional to the shadow radius under the case of the photons uncoupled to the Weyl tensor.

* Xian-Ru Hu: huxianru@lzu.edu.cn

I. INTRODUCTION

Einstein's general theory of relativity predicted the existence of black holes, which has fascinated physicists over decades. Thus it is very important to detect black hole parameters for studying features of the black hole. Investigations show that observing the shadow of black hole provides a tentative way to obtain information as regards black hole [1–8]. In the last few years, the subject of black hole shadow aroused physicists' wide attentions. As we all know, the shadow of black hole is determined by light rays that fall into an event horizon, which depends on the black hole parameters and the interaction between light and other fields. Drummond and Hathrell [9] first found that the superluminal photon propagation in gravitational backgrounds due to vacuum polarisation in QED induces interactions between the electromagnetic field and gravitational field, which has also been studied in Ref. [10–12]. What's more, since light is actually a kind of electromagnetic wave, Ref. [13] has shown that coupling with Weyl tensor breaks the universal relation with the $U(1)$ central charge observed at leading order. Then Songbai Chen *et al.* studied the strong gravitational lensing for the photons coupled to Weyl tensor in black hole spacetimes [14, 15] and Yang Huang first discussed the double shadow of the black hole as photons couple to the Weyl tensor in Ref. [16]. Recently, the coupling of electromagnetic field and gravitational field has been studied widely in Refs. [17, 18]. It indicates that the the interaction between electromagnetic field and gravitational field changes the path of photons propagation and leads to the birefringence phenomenon of light.

On the other hand, the discovery of gravity waves [19] related to compact objects such as black holes, which is one of the outstanding discoveries, has provided us with a new window to understand the universe. It is well known that black hole perturbations result in the emission of gravitational waves, which are characterized

by complex frequencies called quasinormal modes (QNMs). And QNMs have been investigated by using other analytic and numerical methods [20–28]. What’s more, a connection between the shadow of black hole and QNMs has attracted a lot of attention in recent years. Cardoso *et al.* pointed out that in the eikonal limit, the real part of QNMs is connected to the last circular null geodesic in Ref. [29], and Stefanov *et al.* found a connection between the black hole QNMs and the strong gravitation lensing in the strong field regime [30]. Then in a recent work [31], Jusufi explored the relationship between the shadow of nonrotating black hole and QNMs, and pointed out that in the eikonal limit the real part of QNMs is inversely proportional to the shadow radius, which is also applicable in the background of general rotating black holes [32–36]. Therefore, it is very fair and motivating to connect these two properties as they open a new arena in black hole physics. And generalizing this correspondence to a more general case to test its domain of validation is still crucial.

Our aim in this paper is to explore how the shadow of a 4D Einstein-Gauss-Bonnet black hole changes as photons couple to the Weyl tensor. And with above results in mind, we investigate the connection between the shadow radius and QNMs, which is astrophysically relevant and has never been discussed. It is well known that in GB gravity, spherically symmetric black hole solutions exist only in higher dimensions due to the Gauss-Bonnet action does not contribute to the dynamics of the four-dimensional spacetime. Recently, a general covariant GB modified gravity in four dimensions was proposed by rescaling the GB coupling parameter $\hat{\alpha} \rightarrow \frac{\alpha}{D-4}$ which completed the missing piece of the EGB gravity [37]. Such theory can bypass the Lovelock’s theorem and avoid Ostrogradsky instability. A novel 4D static and spherically symmetric black hole solution was obtained while taking the limit $D \rightarrow 4$. However, since the publication of the paper [37], there have appeared several works [38–41] debating that the procedure of taking $D \rightarrow 4$ limit in [37] may not be consistent. On the other hand, some approaches have been proposed either by performing

a regularized Kaluza–Klein reduction [42, 43] or by introducing a counter term into the action [44, 45] to circumvent the issues of the novel 4D EGB gravity. Moreover, a proposal has been suggested in [46], which focuses on temporal diffeomorphism breaking instead of the inclusion of a scalar degree of freedom. Nevertheless, the black-hole solution of [37] also satisfies the field equations of the well-defined theory suggested in [46]. Therefore, the static and spherically symmetric black hole solution itself is meaningful and worthy of studying more deeply. Then, the charged [47] and rotating [48] analogues were obtained for new 4D EGB theory. What’s more, very recently a lot of work has been made, which involved thermodynamics of black hole [49], charged particles and epicyclic motions around 4D EGB black hole [50] and the motions of spinning particles [51].

This paper is organized as follows. In Sec. II, we derive equations of motion for the photons coupled to the Weyl tensor in a 4D Einstein-Gauss-Bonnet black hole spacetime. Then in Sec. III, we further explore the change of the black hole shadow as photons couple to the Weyl tensor. Sec. IV is devoted to studying the QNMs of scalar fields in a 4D Einstein-Gauss-Bonnet black hole spacetime by using the sixth-order WKB method. After that, the connection between the shadow radius and QNMs is investigated in Sec. V. Finally, we comment on our results in Sec. VI

II. EQUATION OF MOTION FOR THE PHOTONS COUPLED TO WEYL TENSOR

In this section, we begin with the action of the electromagnetic field coupled to Weyl tensor in a 4D Einstein-Gauss-Bonnet black hole spacetime, which can be expressed as [13, 37]

$$S = \frac{1}{16\pi G} \int d^D x \sqrt{-g} [R + \frac{\alpha}{D-4} \mathcal{L}_{GB}] + \int d^D x \sqrt{-g} \mathcal{L}_m, \quad (1)$$

where the four-dimensional case is defined as the $D \rightarrow 4$ limit and $\mathcal{L}_{GB} = R_{\mu\nu}^{\rho\sigma}R_{\rho\sigma}^{\mu\nu} - 4R_{\mu}^{\nu}R_{\nu}^{\mu} + R^2$ is the Gauss-Bonnet invariant. $\mathcal{L}_m = -\frac{1}{4}(F_{\mu\nu}F^{\mu\nu} - 4\lambda C^{\mu\nu\rho\sigma}F_{\mu\nu}F_{\rho\sigma})$ is the Lagrangian density of the electromagnetic field coupled to the Weyl tensor in the D-dimensional spacetime and $F_{\mu\nu} = \partial_{\mu}A_{\nu} - \partial_{\nu}A_{\mu}$ is the usual electromagnetic tensor. $C_{\mu\nu\rho\sigma}$ is the Weyl tensor with a form $C_{\mu\nu\rho\sigma} = R_{\mu\nu\rho\sigma} - \frac{2}{(D-2)}(g_{\mu[\rho}R_{\sigma]\nu} - g_{\nu[\rho}R_{\sigma]\mu}) + \frac{2}{(D-1)(D-2)}Rg_{\mu[\rho}g_{\sigma]\nu}$. And the photons coupled to the Weyl tensor can be characterized by the coupling parameter λ . Now considering a four-dimensional spacetime, Varying the action (1) with respect to A_{μ} , we can obtain the corrected Maxwell equation

$$\nabla_{\mu}(F^{\mu\nu} - 4\lambda C^{\mu\nu\rho\sigma}F_{\rho\sigma}) = 0. \quad (2)$$

From the above corrected Maxwell equation (2), one can obtain the equation of motion of the coupled photons by the geometric optics approximation. Under this approximation, $\lambda_c < \lambda < L$, where λ is the wavelength of photon, L is a typical curvature scale, and λ_c is the electron Compton wavelength [10–12, 52–55]. In this method, the electromagnetic field strength can be written as

$$F_{\mu\nu} = f_{\mu\nu}e^{i\theta}, \quad (3)$$

where $f_{\mu\nu}$ is a slowly varying amplitude and θ is a rapidly varying phase. The wave vector is defined as $k_{\mu} = \partial_{\mu}\theta$, which corresponds to the photon momentum in the quantum partical interpretation. According to the Bianchi identity, the amplitude $f_{\mu\nu}$ has the form $f_{\mu\nu} = k_{\mu}a_{\nu} - k_{\nu}a_{\mu}$, where a_{μ} can be interpreted as the polarization vector of photon and satisfies $k_{\mu}a^{\mu} = 0$. Inserting Eq. (3) into Eq. (2) and using the relationship above, we arrive at

$$k_{\mu}k^{\mu}a^{\nu} + 8\lambda C^{\mu\nu\rho\sigma}k_{\sigma}k_{\mu}a_{\rho} = 0. \quad (4)$$

Obviously, the coupling between Wely tensor and electromagnetic field affects the propagation of the coupled photons in the background spacetime.

Let us now consider the 4D Einstein-Gauss-Bonnet black hole obtained by Glavan and Lin in [37], with the metric form

$$ds^2 = -f(r) dt^2 + f(r)^{-1} dr^2 + r^2(d\theta^2 + \sin^2\theta d\phi^2) \quad (5)$$

where

$$f(r) = 1 + \frac{r^2}{2\alpha} \left(1 \pm \sqrt{1 + \frac{8\alpha M}{r^3}}\right). \quad (6)$$

Here, the sign \pm refers to the two different branches, and we consider only the negative branch because it gives a Schwarzschild-like solution in the asymptotically limit [37, 56–60].

Now introduce a local orthonormal frame. The appropriate basis 1-forms are e^a ($a = 0, 1, 2, 3$) with

$$e^0 = \sqrt{f} dt, \quad e^1 = \frac{1}{\sqrt{f}} dr, \quad e^2 = r d\theta, \quad e^3 = r \sin\theta d\phi. \quad (7)$$

Introducing the notation $U_{ab}^{01} = \delta_a^0 \delta_b^1 - \delta_a^1 \delta_b^0$ [9–12], etc., the Weyl tensor can be simplified as

$$C_{abcd} = \mathcal{A}(2U_{ab}^{01}U_{cd}^{01} - U_{ab}^{02}U_{cd}^{02} - U_{ab}^{03}U_{cd}^{03} + U_{ab}^{12}U_{cd}^{12} + U_{ab}^{13}U_{cd}^{13} - 2U_{ab}^{23}U_{cd}^{23}) \quad (8)$$

with

$$\mathcal{A} = -\frac{M(r^3 + 2M\alpha)\sqrt{1 + \frac{8M\alpha}{r^3}}}{(r^3 + 8M\alpha)^2}. \quad (9)$$

To solve the equation of motion of photon, it is convenient to introduce the following linear combination of momentum components [9–12]

$$l_b = k^a U_{ab}^{01}, \quad m_b = k^a U_{ab}^{02}, \quad r_b = k^a U_{ab}^{03}, \quad (10)$$

together with the dependent combinations

$$p_b = k^a U_{ab}^{12}, \quad q_b = k^a U_{ab}^{13}, \quad n_b = k^a U_{ab}^{23}. \quad (11)$$

The equation of motion for the coupled photons (4) can be rewritten as a set of equations for the independent polarisation components $a \cdot l$, $a \cdot m$ and $a \cdot n$. Plugging Eq. (8) into Eq. (4), we therefore arrive at

$$\begin{pmatrix} K_{11} & 0 & 0 \\ K_{21} & K_{22} & K_{23} \\ 0 & 0 & K_{33} \end{pmatrix} \begin{pmatrix} a \cdot l \\ a \cdot m \\ a \cdot n \end{pmatrix} = 0 \quad (12)$$

with

$$\begin{aligned} K_{11} &= (1 - 16\lambda\mathcal{A})(-k^0k^0 + k^1k^1) + (1 + 8\lambda\mathcal{A})(k^2k^2 + k^3k^3), \\ K_{21} &= -24\lambda\mathcal{A}k^1k^2, \\ K_{22} &= (1 + 8\lambda\mathcal{A})(-k^0k^0 + k^1k^1 + k^2k^2 + k^3k^3), \\ K_{23} &= 24\lambda\mathcal{A}k^0k^3, \\ K_{33} &= (1 + 8\lambda\mathcal{A})(-k^0k^0 + k^1k^1) + (1 - 16\lambda\mathcal{A})(k^2k^2 + k^3k^3). \end{aligned} \quad (13)$$

The condition of Eq. (12) with the non-zero solution is $K_{11}K_{22}K_{33} = 0$. The first root $K_{11} = 0$ leads to the modified light cone

$$(1 - 16\lambda\mathcal{A})(-k^0k^0 + k^1k^1) + (1 + 8\lambda\mathcal{A})(k^2k^2 + k^3k^3) = 0, \quad (14)$$

which corresponds to the case of the polarisation vector $a_\mu = \lambda l_\mu$. The second root $K_{22} = 0$ corresponds to an unphysical polarisation and should be neglected. The third root is $K_{33} = 0$, i.e.,

$$(1 + 8\lambda\mathcal{A})(-k^0k^0 + k^1k^1) + (1 - 16\lambda\mathcal{A})(k^2k^2 + k^3k^3) = 0, \quad (15)$$

which means that the vector $a_\mu = \lambda n_\mu$.

The above discussion shows that the light cone condition depends not only on the coupling between the photon and the Weyl tensor, but also on the polarization

of light. We know from Eqs. (14) and (15) that the velocities of the photons for the two polarizations are different, i.e., the phenomenon of gravitational birefringence. Moreover, the light cone conditions (14) and (15) imply that instead of following geodesic in the original metric, the coupled photons follow null geodesics of the effective metric $\gamma_{\mu\nu}$, i.e., $\gamma^{\mu\nu}k_\mu k_\nu = 0$ [61]. The effective metric for the coupled photon can be expressed as

$$ds^2 = -f(r) dt^2 + f(r)^{-1} dr^2 + r^2 W(r)^{-1} (d\theta^2 + \sin^2\theta d\phi^2). \quad (16)$$

The quantity $W(r)$ is

$$W(r) = \frac{r^6 \sqrt{1 + \frac{8M\alpha}{r^3}} + Mr^3(8\alpha\sqrt{1 + \frac{8M\alpha}{r^3}} - 8\lambda) - 16M^2\alpha\lambda}{r^6 \sqrt{1 + \frac{8M\alpha}{r^3}} + 32M^2\alpha\lambda + Mr^3(8\alpha\sqrt{1 + \frac{8M\alpha}{r^3}} + 16\lambda)}, \quad (17)$$

for photon with the polarization along $l_\mu(PPL)$, it is

$$W(r) = \frac{r^6 \sqrt{1 + \frac{8M\alpha}{r^3}} + 32M^2\alpha\lambda + Mr^3(8\alpha\sqrt{1 + \frac{8M\alpha}{r^3}} + 16\lambda)}{r^6 \sqrt{1 + \frac{8M\alpha}{r^3}} + Mr^3(8\alpha\sqrt{1 + \frac{8M\alpha}{r^3}} - 8\lambda) - 16M^2\alpha\lambda}, \quad (18)$$

for photon with the polarization along $n_\mu(PPN)$ [16].

III. WEYL CORRECTIONS TO SHADOW RADIUS

In this subsection, we will discuss the shadow radius of black hole as photons couple to the Weyl tensor. In the effective metric (16), there exist two conserved quantities energy E and angular momentum L as follow

$$E = f(r)\dot{t}, \quad L = r^2 \sin^2\theta W(r)^{-1} \dot{\phi}, \quad (19)$$

where the dot over a symbol is the differentiation with respect to an affine parameter β . Using the condition $\gamma^{\mu\nu}k_\mu k_\nu = 0$ and $k_\mu = \frac{dx_\mu}{d\beta}$, one can obtain the equations of

motion

$$\frac{r^4 \dot{r}^2}{W(r)^2} = R(r), \quad (20)$$

$$\frac{r^4 \dot{\theta}^2}{W(r)^2} = \Theta(\theta). \quad (21)$$

Here, $R(r)$ and $\Theta(\theta)$ are given by

$$R(r) = \frac{E^2 r^4}{W(r)^2} - \frac{(\mathcal{Q} + L^2) r^2 f(r)}{W(r)}, \quad (22)$$

$$\Theta(\theta) = \mathcal{Q} - L^2 \cot^2 \theta, \quad (23)$$

with \mathcal{Q} denoting the Carter constant [62]. To determine the geometric shape of the shadow of the effective metric, using the unstable condition

$$R(r) = 0, \quad \frac{dR(r)}{dr} = 0, \quad \frac{d^2 R(r)}{dr^2} > 0, \quad (24)$$

one can obtain that

$$2f(r)W(r) - rf'(r)W(r) - rf(r)W'(r) = 0. \quad (25)$$

By solving this equation, one can determine the radius of the photon sphere r_{ps} . In particular, combining Eq. (24) with celestial coordinates [63]

$$x = \lim_{r_i \rightarrow \infty} \left(-r_i^2 \sin \theta_i \frac{d\phi}{dr} \right) \Big|_{(r_i, \theta_i)}, \quad y = \lim_{r_i \rightarrow \infty} \left(r_i^2 \frac{d\theta}{dr} \right) \Big|_{(r_i, \theta_i)}, \quad (26)$$

one can express the radius of the shadow R_{sh} of the effective metric by the simple relation

$$R_{sh} = \sqrt{x^2 + y^2} = \frac{r_{ps}}{\sqrt{W(r_{ps})f(r_{ps})}}, \quad (27)$$

while taking the limit $r_i \rightarrow \infty$ according to the location of the observer and assuming the observer is situated in the equatorial plane ($\theta_i = \frac{\pi}{2}$).

Considering that a photon should propagate continuously in the region outside the event horizon r_+ , the coupling constant λ must satisfy $r_+^6 \sqrt{1 + \frac{8M\alpha}{r_+^3}} +$

α	r_+	r_{ps}/R_{sh} (PPL)			r_{ps}/R_{sh} (PPN)		
		$\lambda = 0.2$	$\lambda = 0$	$\lambda = -0.2$	$\lambda = 0.2$	$\lambda = 0$	$\lambda = -0.2$
0.2	1.894	3.155/5.535	2.907/5.116	2.639/4.594	2.675/4.636	2.907/5.116	3.179/5.554
0.4	1.775	3.049/5.452	2.803/5.029	2.550/4.513	2.583/4.553	2.803/5.029	3.075/5.471
0.5	1.707	2.992/5.407	2.747/4.982	2.500/4.469	2.532/4.508	2.747/4.982	3.017/5.428
0.6	1.632	2.930/5.361	2.686/4.932	2.445/4.421	2.476/4.460	2.686/4.932	2.957/5.382
0.8	1.447	2.791/5.259	2.547/4.823	2.315/4.313	2.345/4.352	2.547/4.823	2.819/5.281
1	1	2.622/5.142	2.372/4.694	2.140/4.178	2.170/4.219	2.372/4.694	2.654/5.166

Table I: The event horizon r_+ , photon sphere radius r_{ps} and shadow radius R_{sh} with different GB coupling constant α in a 4D Einstein-Gauss-Bonnet black hole spacetime.

$32M^2\alpha\lambda + Mr_+^3(8\alpha\sqrt{1 + \frac{8M\alpha}{r_+^3}} + 16\lambda) > 0$ for PPL and satisfy $r_+^6\sqrt{1 + \frac{8M\alpha}{r_+^3}} + Mr_+^3(8\alpha\sqrt{1 + \frac{8M\alpha}{r_+^3}} - 8\lambda) - 16M^2\alpha\lambda > 0$ for PPN. With this constraint, setting $M = 1$, the range of the GB coupling parameter α is chosen in $0 < \alpha \leq 1$ and the coupling constant λ is limited in the range $\lambda \in [-0.2, 0.2]$, such that the condition $r_+ < r_{ps} < R_{sh}$ holds [64], seeing Table I. Obviously, due to the complex dependence of the equation (25) on the GB coupling parameter α and the coupling constant λ , we can not get an analytical form for the photon sphere radius for the coupled photons, so the computational way is chosen. With the help of the numerical method, we can get the variation of R_{sh} with parameter λ of the photons coupled to the Weyl tensor and the GB coupling constant α for PPL and PPN, and the results are shown in Figs. 1 and 2.

In Fig. 1, it tells us that with the increase of the coupling parameter λ , the shadow radius R_{sh} for different values of α increases for PPL and decreases for PPN.

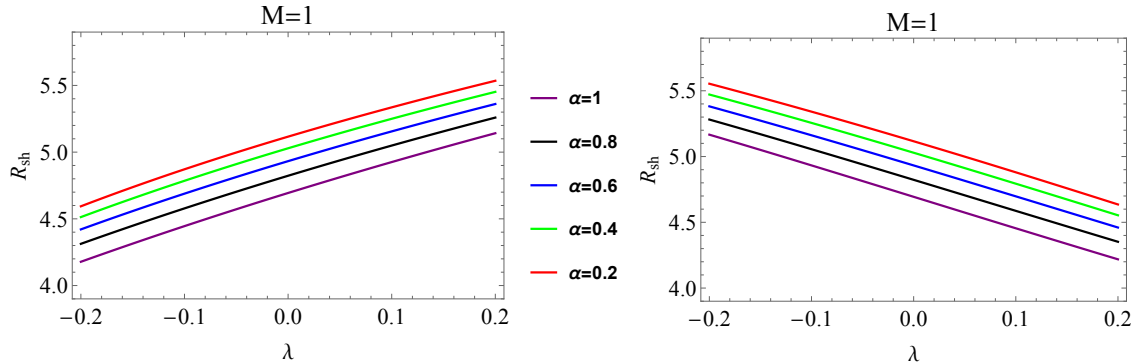


Figure 1: Variation of the shadow radius R_{sh} with the coupling parameter λ in a 4D Einstein-Gauss-Bonnet black hole spacetime. The left and the right are for PPL and PPN, respectively.

However, as $\lambda \rightarrow 0$, $W(r) \rightarrow 1$, the equation of circular photon orbits for PPL is the same as that for PPN, and the solution (16) reduces to the 4D Einstein-Gauss-Bonnet black hole with the shadow investigated in [65]. The variation of the shadow radius with the GB coupling parameter α in our article is consistent with the result in [65]. In addition, one can find that the shadow depends not only on the properties of background black hole spacetime, but also on the polarization of the coupled photons. Moreover, with the increase of the GB coupling parameter α , the shadow radius R_{sh} decreases for different polarizations of photons in Fig. 2. The shadow radius R_{sh} of PPL is different from that of PPN in Fig. 2 for fixed value of λ , which means the birefringence phenomenon occurs exactly in this case with non-vanishing λ . When $\alpha \rightarrow 0$, the R_{sh} reduces to the radius of the shadow for the photons coupled to Weyl tensor in a Schwarzschild black hole spacetime which has been studied in [14]. It indicates that with increase of λ , the shadow radius R_{sh} increases for PPL and decreases for PPN in the Schwarzschild black hole spacetime, which is consistent with our result. We also find that the shadow radius in the 4D Einstein-Gauss-

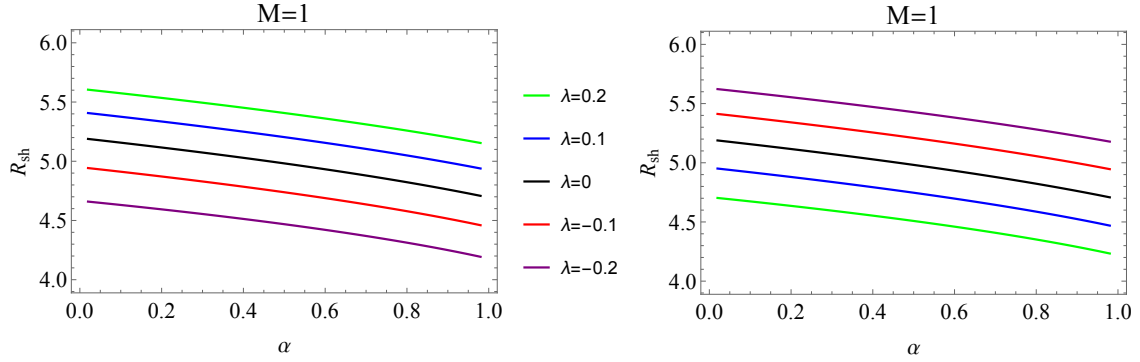


Figure 2: Variation of the shadow radius R_{sh} with the GB coupling parameter α in a 4D Einstein-Gauss-Bonnet black hole spacetime. The left and right are for PPL and PPN, respectively.

Bonnet black hole spacetime is always smaller than that in Schwarzschild black hole spacetime for the GB coupling constant $0 < \alpha \leq 1$.

IV. QNMS OF SCALAR FIELD

Considering a massless scalar field perturbation in the metric (5), it satisfies the Klein-Gorden equation

$$\frac{1}{\sqrt{-g}}\partial_{\mu}(\sqrt{-g}g^{\mu\nu}\partial_{\nu}\Phi) = 0. \quad (28)$$

Involving a separation of variables, the function Φ for the scalar field is given in terms of the spherical harmonics

$$\Phi(t, r, \theta, \phi) = \frac{1}{r}e^{-i\omega t}Y_l(\theta, \phi)\Psi(r), \quad (29)$$

in which $e^{-i\omega t}$ represents the time evolution of the field. Inserting Eq. (29) into Eq. (28) and introducing a "tortoise" coordinate $dr_* = \frac{dr}{f(r)}$, we can show that the field perturbation equation is given by the Schrödinger wave-like equation

$$\frac{d^2\Psi}{dr_*^2} + (\omega^2 - V_S(r))\Psi = 0. \quad (30)$$

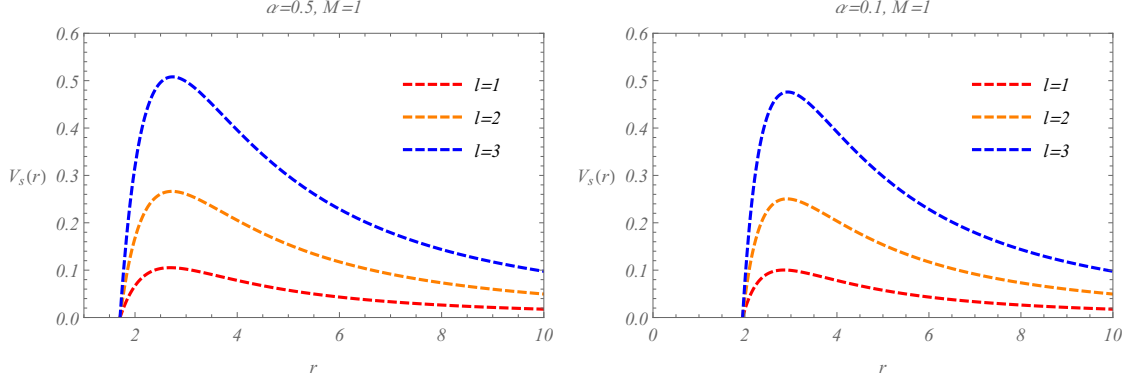


Figure 3: The figures are the effective potentials of the scalar field perturbation V_S for different values of the GB coupling constant α . Changing the parameter α changes the height of the potential barrier.

Under the positive real part, QNMs, by definition, satisfy the following boundary condition,

$$\Psi(r_*) = C_{\pm} \exp(\pm i\omega r_*), \quad r \rightarrow \infty \quad (31)$$

where ω can be further written in terms of the real and imaginary parts, i.e., $\omega = \omega_R - i\omega_I$. The real and imaginary parts of QNMs represent the oscillation frequency and the decay rate, respectively. The effective potential $V_S(r)$ in Eq. (30) can be written as

$$V_S(r) = \left[1 + \frac{r^2}{2\alpha} \left(1 - \sqrt{1 + \frac{8\alpha M}{r^3}} \right) \right] \times \left[\frac{l(l+1)}{r^2} - \frac{2\alpha + r^3 \sqrt{1 + \frac{8\alpha M}{r^3}}}{\alpha r^3 \sqrt{1 + \frac{8\alpha M}{r^3}}} \right], \quad (32)$$

where l denotes the multipole number. One can deduce from Fig. 3 that the height of the potential barrier governed by the effective potential increases with multipole number l and the GB coupling parameter α . With the expression of the effective potential in hand, one can use the WKB approach to compute the QNM frequencies.

spin 0	l=1, n=0	l=2, n=0	l=2, n=1
α	$\omega(\text{WKB})$	$\omega(\text{WKB})$	$\omega(\text{WKB})$
0.2	$0.2977 - 0.0948i$	$0.4914 - 0.0936i$	$0.4736 - 0.2853i$
0.4	$0.3028 - 0.0912i$	$0.5000 - 0.0899i$	$0.4839 - 0.2734i$
0.5	$0.3057 - 0.0891i$	$0.5048 - 0.0877i$	$0.4892 - 0.2665i$
0.6	$0.3087 - 0.0867i$	$0.5099 - 0.0853i$	$0.4947 - 0.2588i$
0.8	$0.3154 - 0.0806i$	$0.5211 - 0.0795i$	$0.5057 - 0.2399i$
1	$0.3227 - 0.0723i$	$0.5343 - 0.0711i$	$0.5146 - 0.2147i$

Table II: The real and imaginary parts of quasinormal frequencies of the scalar field in the 4D Einstein-Gauss-Bonnet black hole spacetime with different coupling constant α .

This method was proposed by Schutz and Will [20], then Iyer and Will extended the first order WKB formula to the third order [25]. In the present paper, we shall use the sixth-order WKB method which is described in [26] for calculating QNMs. We have presented the values of the QNMs for the scalar perturbation in Table II.

From Table II, we find that with the increase of the GB coupling parameter α , the real part of QNMs increases and the imaginary part decreases in absolute value. This particular effect can be clearly seen in Fig. 4. Moreover, we also see that higher absolute values of ω_I are obtained for the case $l = 2$ and $n = 1$, which means the scalar field perturbation damps more rapidly. It is worth noting that the WKB method works for $l > n$ (where n is the overtone number), otherwise, the accuracy is worse. So that we have not calculated the QNMs for the fundamental mode $l = 0, n = 0$, but can use the Frobenius method [66].

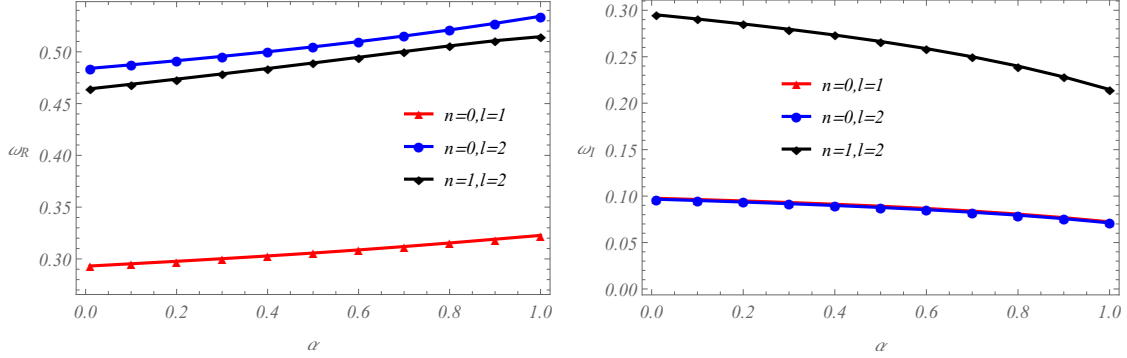


Figure 4: Left panel: Plots of the real part of the QNMs versus the GB coupling parameter α for the scalar field. Right panel: Plots of the imaginary part of QNMs versus the GB coupling parameter α . In both cases we have chosen $M = 1$.

V. CONNECTION BETWEEN THE SHADOW RADIUS AND QNMS

At high l , the WKB formula found in [20, 25, 26] can be applied for finding quasinormal modes

$$\frac{Q_0(r_0)}{\sqrt{2Q_0^{(2)}(r_0)}} = i(n + 1/2), \quad (33)$$

where $Q_0^{(2)} = \frac{d^2 Q_0}{dr_*^2}$ is evaluated at the extremum r_0 of the function Q_0 . In the eikonal limit for perturbations

$$Q_0 \simeq \omega^2 - f(r) \frac{l^2}{r^2}, \quad (34)$$

one can find that the extremum of Q_0 satisfies $2f(r_0) - r_0 f'(r_0) = 0$, which coincides with Eq. (25) in the case of $\lambda = 0$ i.e. the position of the effective potential's extremum r_0 coincides with the location of the unmodified unstable photon orbit r_{ps} . Then, there is a main result drawn by Cardoso *et al.* [29]. In the eikonal approximation, for any spherically symmetric spacetimes, the real part of the QNMs is given by the angular velocity of the unstable circular null geodesics while the

imaginary part of the QNMs is related to the instability time scale of the orbit that can be represented by the Lyapunov exponent η

$$\omega = \Omega l - i(n + 1/2)|\eta|. \quad (35)$$

Here, Ω and η are given by

$$\Omega = \frac{\sqrt{f(r_{ps})}}{r_{ps}}, \quad (36)$$

$$\eta = \sqrt{\frac{f(r_{ps})(2f(r_{ps}) - r_{ps}^2 f''(r_{ps}))}{2r_{ps}^2}}, \quad (37)$$

with r_{ps} is the unmodified photon sphere radius. What's more, Stefanov *et al.* published a paper in 2010 [30], which pointed out a connection between the black hole QNMs and the strong gravitation lensing in the strong field regime. In recent years, Jusufi found that in the eikonal limit the real part of QNMs is inversely proportional to the shadow radius [31–33]

$$\omega_R \propto \frac{1}{R_{sh}}. \quad (38)$$

Further, the relationship between the real part of QNMs and the shadow radius can be expressed as

$$\omega_R = \lim_{l \gg 1} \frac{l}{R_{sh}}, \quad (39)$$

which is precise in the eikonal limit having large values of l under the case of the photons uncoupled to the Weyl tensor. By this relationship, one obtains that the unmodified shadow radius decreases with the increase of the GB coupling constant α as the real part of QNMs increases. This effect is indeed shown to be the case in Figs. 2 and 4. Besides, from Table I and Table II, one can find the numerical results are consistent with Eq. (39) approximately. It can be interpreted as the fact that

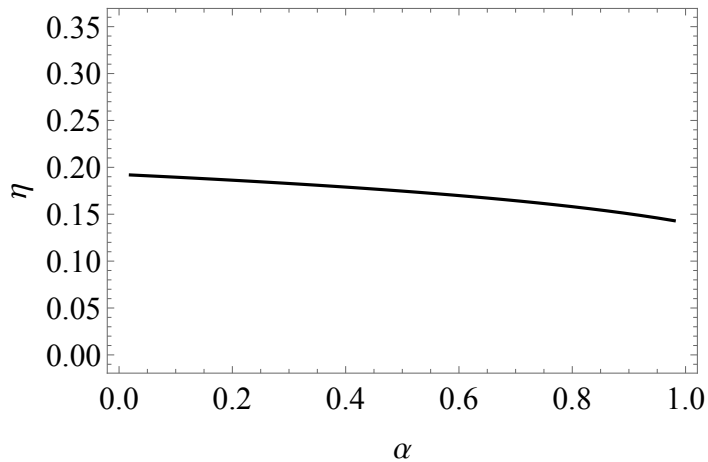


Figure 5: Plot of the Lyapunov exponent η versus the GB coupling parameter α . In this cases we have chosen $M = 1$.

a decrease of the black hole horizon leads to a decrease of the shadow radius and consequently higher values for the oscillation frequencies. In addition, the Lyapunov exponent η is shown for the 4D Einstein-Gauss-Bonnet black hole in Fig. 5. One can find that the variation of the Lyapunov exponent η with the GB coupling parameter α in Fig. 5 is consistent with that of ω_I with α in Fig. 4

VI. CONCLUSION

In this paper, we have studied the shadow of a 4D Einstein-Gauss-Bonnet black hole as the photons couple to Weyl tensor and pointed out a simple connection between the shadow radius and the real part of QNMs. We found that the shadow of black hole depends not only on the GB coupling constant α , but also on the coupling parameter λ and the polarization of photon. For different polarizations of photon, the shadow radius R_{sh} decreases as the GB coupling constant α increases. However, with a increase of the coupling parameter λ , the shadow radius R_{sh} increases for

PPL and decreases for PPN.

Moreover, the connection between the shadow radius and the real part of QNMs satisfies Eq. (39) while taking $\lambda = 0$ in the spacetime background of a 4D Einstein-Gauss-Bonnet black hole. Computing the QNM frequencies for the scalar field perturbation by the sixth-order WKB approach, we found that the real part of QNMs increases with the increase of the GB coupling constant α . Then using the correspondence between the geodesics and quasinormal spectrum, we pointed out the relationship between the shadow radius and the real part of QNMs under the case of the photons uncoupled to the Weyl tensor. We have also applied the unmodified unstable photon orbit of the black hole to compute the imaginary part of the QNM frequencies in the eikonal limit. This may imply a potential connection between the shadow of black hole and gravitational wave. Recently, the result that the size of the shadow can reflect the phase structure of the axially symmetric black hole was explored in Ref. [67]. This suggests that QNMs in connection with the thermodynamic phase structure of the black hole and our work opens an avenue for exploring this connection.

CONFLICTS OF INTEREST

The authors declare that there are no conflicts of interest regarding the publication of this paper.

ACKNOWLEDGMENTS

We would like to thank the National Natural Science Foundation of China (Grant No.11571342) for supporting us on this work.

REFERENCES

- [1] JL Synge. The escape of photons from gravitationally intense stars. *Monthly Notices of the Royal Astronomical Society*, 131(3):463–466, 1966.
- [2] ID Novikov and KS Thorne. Black Holes,(edited by C. deWitt and B. deWitt), 1973.
- [3] Subrahmanyan Chandrasekhar and Subrahmanyan Chandrasekhar. *The mathematical theory of black holes*, volume 69. Oxford University Press, 1998.
- [4] Zdeněk Stuchlík, Daniel Charbulák, and Jan Schee. Light escape cones in local reference frames of Kerr–de Sitter black hole spacetimes and related black hole shadows. *The European Physical Journal C*, 78(3):1–32, 2018.
- [5] Arne Grenzebach, Volker Perlick, and Claus Lämmerzahl. Photon regions and shadows of accelerated black holes. *International Journal of Modern Physics D*, 24(09):1542024, 2015.
- [6] Farruh Atamurotov, Ahmadjon Abdujabbarov, and Bobomurat Ahmedov. Shadow of rotating non-Kerr black hole. *Physical Review D*, 88(6):064004, 2013.
- [7] Sunny Vagnozzi and Luca Visinelli. Hunting for extra dimensions in the shadow of M87. *Physical Review D*, 100(2):024020, 2019.
- [8] Tian-Chi Ma, He-Xu Zhang, Peng-Zhang He, Hao-Ran Zhang, Yuan Chen, and Jian-Bo Deng. Shadow cast by a rotating and nonlinear magnetic-charged black hole in perfect fluid dark matter. *Modern Physics Letters A*, page 2150112, 2021.
- [9] Ian T Drummond and SJ Hathrell. QED vacuum polarization in a background gravitational field and its effect on the velocity of photons. *Physical Review D*, 22(2):343, 1980.

- [10] RD Daniels and Graham M Shore. “Faster than light” photons and charged black holes. *Nuclear Physics B*, 425(3):634–650, 1994.
- [11] RD Daniels and Graham M Shore. “Faster than light” photons and rotating black holes. *Physics Letters B*, 367(1-4):75–83, 1996.
- [12] Rong-Gen Cai. Propagation of vacuum polarized photons in topological black hole spacetimes. *Nuclear Physics B*, 524(3):639–657, 1998.
- [13] Adam Ritz and John Ward. Weyl corrections to holographic conductivity. *Physical Review D*, 79(6):066003, 2009.
- [14] Songbai Chen and Jiliang Jing. Strong gravitational lensing for the photons coupled to Weyl tensor in a Schwarzschild black hole spacetime. *Journal of Cosmology and Astroparticle Physics*, 2015(10):002, 2015.
- [15] Songbai Chen, Shangyun Wang, Yang Huang, Jiliang Jing, and Shiliang Wang. Strong gravitational lensing for the photons coupled to a Weyl tensor in a Kerr black hole spacetime. *Physical Review D*, 95(10):104017, 2017.
- [16] Yang Huang, Songbai Chen, and Jiliang Jing. Double shadow of a regular phantom black hole as photons couple to the Weyl tensor. *The European Physical Journal C*, 76(11):1–7, 2016.
- [17] He-Xu Zhang, Cong Li, Peng-Zhang He, Qi-Qi Fan, and Jian-Bo Deng. Optical properties of a Brane-World black hole as photons couple to the Weyl tensor. *The European Physical Journal C*, 80:1–11, 2020.
- [18] Songbai Chen, Mingzhi Wang, and Jiliang Jing. Polarization effects in Kerr black hole shadow due to the coupling between photon and bumblebee field. *Journal of High Energy Physics*, 2020(7):1–17, 2020.
- [19] Benjamin P Abbott, Richard Abbott, TD Abbott, MR Abernathy, Fausto Acernese, Kendall Ackley, Carl Adams, Thomas Adams, Paolo Addesso, RX Adhikari, et al. Observation of gravitational waves from a binary black hole merger. *Physical Review*

- Letters*, 116(6):061102, 2016.
- [20] Bernard F Schutz and Clifford M Will. Black hole normal modes: a semianalytic approach. *The Astrophysical Journal*, 291:L33–L36, 1985.
- [21] Valeria Ferrari and Bahram Mashhoon. New approach to the quasinormal modes of a black hole. *Physical Review D*, 30(2):295, 1984.
- [22] Subrahmanyan Chandrasekhar and Steven Detweiler. The quasi-normal modes of the Schwarzschild black hole. *Proceedings of the Royal Society of London. A. Mathematical and Physical Sciences*, 344(1639):441–452, 1975.
- [23] Edward W Leaver. An analytic representation for the quasi-normal modes of Kerr black holes. *Proceedings of the Royal Society of London. A. Mathematical and Physical Sciences*, 402(1823):285–298, 1985.
- [24] Gary T Horowitz and Veronika E Hubeny. Quasinormal modes of AdS black holes and the approach to thermal equilibrium. *Physical Review D*, 62(2):024027, 2000.
- [25] Sai Iyer and Clifford M Will. Black-hole normal modes: A WKB approach. I. Foundations and application of a higher-order WKB analysis of potential-barrier scattering. *Physical Review D*, 35(12):3621, 1987.
- [26] RA Konoplya. Quasinormal behavior of the D-dimensional Schwarzschild black hole and the higher order WKB approach. *Physical Review D*, 68(2):024018, 2003.
- [27] Emanuele Berti, Vitor Cardoso, and Andrei O Starinets. Quasinormal modes of black holes and black branes. *Classical and Quantum Gravity*, 26(16):163001, 2009.
- [28] Almendra Aragón, Ramón Bécar, PA González, and Yerko Vásquez. Perturbative and nonperturbative quasinormal modes of 4D Einstein–Gauss–Bonnet black holes. *The European Physical Journal C*, 80(8):1–9, 2020.
- [29] Vitor Cardoso, Alex S Miranda, Emanuele Berti, Helvi Witek, and Vilson T Zanchin. Geodesic stability, Lyapunov exponents, and quasinormal modes. *Physical Review D*, 79(6):064016, 2009.

- [30] Ivan Zh Stefanov, Stoytcho S Yazadjiev, and Galin G Gyulchev. Connection between black-hole quasinormal modes and lensing in the strong deflection limit. *Physical Review Letters*, 104(25):251103, 2010.
- [31] Kimet Jusufi. Quasinormal modes of black holes surrounded by dark matter and their connection with the shadow radius. *Physical Review D*, 101(8):084055, 2020.
- [32] Kimet Jusufi. Connection between the shadow radius and quasinormal modes in rotating spacetimes. *Physical Review D*, 101(12):124063, 2020.
- [33] Kimet Jusufi, Muhammed Amir, Md Sabir Ali, and Sunil D Maharaj. Quasinormal modes, shadow, and greybody factors of 5D electrically charged Bardeen black holes. *Physical Review D*, 102(6):064020, 2020.
- [34] Cheng Liu, Tao Zhu, Qiang Wu, Kimet Jusufi, Mubasher Jamil, Mustapha Azreg-Ainou, and Anzhong Wang. Shadow and quasinormal modes of a rotating loop quantum black hole. *Physical Review D*, 101(8):084001, 2020.
- [35] M Ghasemi-Nodehi, Mustapha Azreg-Ainou, Kimet Jusufi, and Mubasher Jamil. Shadow, quasinormal modes, and quasiperiodic oscillations of rotating Kaluza-Klein black holes. *Physical Review D*, 102(10):104032, 2020.
- [36] Huan Yang. Relating black hole shadow to quasinormal modes for rotating black holes. *Physical Review D*, 103(8):084010, 2021.
- [37] Dražen Glavan and Chunshan Lin. Einstein-Gauss-Bonnet gravity in four-dimensional spacetime. *Physical Review Letters*, 124(8):081301, 2020.
- [38] Wen-Yuan Ai. A note on the novel 4D Einstein–Gauss–Bonnet gravity. *Communications in Theoretical Physics*, 72(9):095402, 2020.
- [39] Fu-Wen Shu. Vacua in novel 4D Einstein-Gauss-Bonnet Gravity: pathology and instability? *Physics Letters B*, 811:135907, 2020.
- [40] Julio Arrechea, Adrià Delhom, and Alejandro Jiménez-Cano. Inconsistencies in four-dimensional Einstein-Gauss-Bonnet gravity. *Chinese Physics C*, 45(1):013107, 2021.

- [41] Julio Arrechea, Adrià Delhom, and Alejandro Jiménez-Cano. Yet another comment on four-dimensional Einstein-Gauss-Bonnet gravity. *arXiv preprint arXiv:2004.12998*, 2020.
- [42] H Lü and Yi Pang. Horndeski gravity as $D \rightarrow 4$ limit of Gauss-Bonnet. *Physics Letters B*, 809:135717, 2020.
- [43] Tsutomu Kobayashi. Effective scalar-tensor description of regularized Lovelock gravity in four dimensions. *Journal of Cosmology and Astroparticle Physics*, 2020(07):013, 2020.
- [44] Pedro GS Fernandes, Pedro Carrilho, Timothy Clifton, and David J Mulryne. Derivation of regularized field equations for the Einstein-Gauss-Bonnet theory in four dimensions. *Physical Review D*, 102(2):024025, 2020.
- [45] Robie A Hennigar, David Kubizňák, Robert B Mann, and Christopher Pollack. On taking the $D \rightarrow 4$ limit of Gauss-Bonnet gravity: theory and solutions. *Journal of High Energy Physics*, 2020(7):1–18, 2020.
- [46] Katsuki Aoki, Mohammad Ali Gorji, and Shinji Mukohyama. A consistent theory of $D \rightarrow 4$ Einstein-Gauss-Bonnet gravity. *Physics Letters B*, 810:135843, 2020.
- [47] Pedro GS Fernandes. Charged black holes in AdS spaces in 4D Einstein Gauss-Bonnet gravity. *Physics Letters B*, 805:135468, 2020.
- [48] Rahul Kumar and Sushant G Ghosh. Rotating black holes in 4D Einstein-Gauss-Bonnet gravity and its shadow. *Journal of Cosmology and Astroparticle Physics*, 2020(07):053, 2020.
- [49] Dharm Veer Singh and Sanjay Siwach. Thermodynamics and Pv criticality of Bardeen-AdS black hole in 4D Einstein-Gauss-Bonnet gravity. *Physics Letters B*, 808:135658, 2020.
- [50] Sanjar Shaymatov, Jaroslav Vrba, Daniele Malafarina, Bobomurat Ahmedov, and Zdeněk Stuchlík. Charged particle and epicyclic motions around 4D Einstein–Gauss–

- Bonnet black hole immersed in an external magnetic field. *Physics of the Dark Universe*, 30:100648, 2020.
- [51] Yu-Peng Zhang, Shao-Wen Wei, and Yu-Xiao Liu. Spinning test particle in four-dimensional Einstein–Gauss–Bonnet black holes. *Universe*, 6(8):103, 2020.
- [52] Graham M Shore. Faster than light photons in gravitational fields II.: Dispersion and vacuum polarisation. *Nuclear Physics B*, 633(1-2):271–294, 2002.
- [53] Hing Tong Cho. “Faster than light” photons in dilaton black hole spacetimes. *Physical Review D*, 56(10):6416, 1997.
- [54] VA De Lorenci, Renato Klippert, M Novello, and JM Salim. Light propagation in non-linear electrodynamics. *Physics Letters B*, 482(1-3):134–140, 2000.
- [55] Diego AR Dalvit, Francisco D Mazzitelli, and Carmen Molina-Paris. One-loop graviton corrections to Maxwell’s equations. *Physical Review D*, 63(8):084023, 2001.
- [56] Timothy Clifton, Pedro Carrilho, Pedro GS Fernandes, and David J Mulryne. Observational constraints on the regularized 4D Einstein-Gauss-Bonnet theory of gravity. *Physical Review D*, 102(8):084005, 2020.
- [57] Minyong Guo and Peng-Cheng Li. Innermost stable circular orbit and shadow of the 4 D Einstein–Gauss–Bonnet black hole. *The European Physical Journal C*, 80(6):1–8, 2020.
- [58] RA Konoplya and AF Zinhailo. Quasinormal modes, stability and shadows of a black hole in the 4D Einstein–Gauss–Bonnet gravity. *The European Physical Journal C*, 80(11):1–13, 2020.
- [59] Cheng-Yong Zhang, Peng-Cheng Li, and Minyong Guo. Greybody factor and power spectra of the Hawking radiation in the 4 D Einstein–Gauss–Bonnet de-Sitter gravity. *The European Physical Journal C*, 80(9):1–9, 2020.
- [60] Si-Jiang Yang, Jun-Jie Wan, Jing Chen, Jie Yang, and Yong-Qiang Wang. Weak cosmic censorship conjecture for the novel 4 D charged Einstein–Gauss–Bonnet black

- hole with test scalar field and particle. *The European Physical Journal C*, 80(10):1–11, 2020.
- [61] Oliver Preuss, Mark P Haugan, Sami K Solanki, and Stefan Jordan. An astronomical search for evidence of new physics: Limits on gravity-induced birefringence from the magnetic white dwarf RE J0317-853. *Physical Review D*, 70(6):067101, 2004.
- [62] Brandon Carter. Global structure of the Kerr family of gravitational fields. *Physical Review*, 174(5):1559, 1968.
- [63] Samuel E Vazquez and Ernesto P Esteban. Strong field gravitational lensing by a Kerr black hole. *arXiv preprint gr-qc/0308023*, 2003.
- [64] H Lu and Hong-Da Lyu. On the size of a black hole: the Schwarzschild is the biggest. *arXiv preprint arXiv:1911.02019*, 2019.
- [65] B Eslam Panah, Kh Jafarzade, and SH4187290 Hendi. Charged 4D Einstein-Gauss-Bonnet-AdS black holes: Shadow, energy emission, deflection angle and heat engine. *Nuclear Physics B*, 961:115269, 2020.
- [66] RA Konoplya, Zdeněk Stuchlík, and A Zhidenko. Massive nonminimally coupled scalar field in Reissner-Nordström spacetime: Long-lived quasinormal modes and instability. *Physical Review D*, 98(10):104033, 2018.
- [67] Ming Zhang and Minyong Guo. Can shadows reflect phase structures of black holes? *The European Physical Journal C*, 80(8):1–9, 2020.